An Oblique Fiber Bundle Test and Analysis

Ning Pan, Yiping Lin, Xungai Wang and Ron Postle

Textile Research Journal 2000; 70; 671
DOI: 10.1177/004051750007000803

An Oblique Fiber Bundle Test and Analysis

NING PAN AND YIPING LIN

Division of Textiles and Clothing, University of California, Davis, California 95616, U.S.A.

XUNGAI WANG

School of Engineering Technology, Deakin University, Geelong, Victoria 3217, Australia

RON POSTLE

Department of Textile Technology, University of New South Wales, Sydney 2052, Australia

ABSTRACT

Although it is widely known to textile scientists that when yarn twist exceeds the optimal level, yarn strength will decline due to the so-called obliquity effect, the exact physical mechanism behind this obliquity effect is still unknown. It is therefore our objective to investigate this issue. We adopt a special technique for tensile sample preparation in which parallel fibers are adhered to a transparent adhesive tape. The angle between the fiber direction and the loading direction can therefore be altered so that the mechanical behavior of the fibers at different loading angles can be observed. The effects of different loading angles on the strengths and breaking strains of the specimens are recorded, thus shedding light on the physics of the obliquity effect.

It has become common knowledge, at least to textile scientists, that yarn strength is a function of the twist inserted into the yarn. For staple yarns, it is easy to understand that there will be no strength in the yarn prior to twisting. As the twist increases, so does the yarn strength. There exists an optimal twist level at which the yarn strength reaches its maximum. Beyond this level, however, yarn strength decreases, attributed to the so-called "fiber obliquity" phenomenon. This effect exists in filament yarns as well. Although the effect has been discussed, for example, by Hearle *et al.* [3], the exact physical reason has not been given. An intuitive explanation for this fiber obliquity effect is that when the twist level exceeds the optimal value, the inclinations or angles between the fiber axes and the yarn axis become so large that a simple force resolution analysis indicates the contribution of fiber strength to yarn strength decreases to such a degree that yarn strength as a whole degrades.

However, another more plausible explanation for the fiber obliquity phenomenon is that a fiber becomes weaker when loaded in an inclined form, *i.e.*, when the tensile force is at an angle with the fiber axis. Of course, such a loading arrangement is against convention, because fibers can only carry a load in their axial direction, and the conventional tensile sample will not do the job; once mounted onto the tensile tester, the originally inclined fiber will first re-orient into a straight format before it can be elongated. To overcome this problem, we use a new kind of specimen, which we introduced recently [8], with a little alternation: a fiber reinforced material is formed in which individual fibers in parallel are adhered to a transparent adhesive tape so that the fibers "bond with" the tape after sufficient curing.

In such a sample, fibers can be arranged in other directions than parallel to the testing direction. In other words, an oblique fiber test is possible. This kind of off-axis test has also been used for composites [2, 4–7].

Materials

For this study, we selected four different fiber types, including polypropylene (PP), polyester (PET), glass, and Kevlar 49, ranging from ductile to brittle. We used 3M Scotch tape (Magic Tape 810EG) to prepare the testing specimens. In order to facilitate the study, we arranged the fibers into parallel bundles before adhering them to the Scotch tape. The specifications of the materials are provided in Tables I and II.

Each parallel fiber bundle was then carefully adhered to the Scotch tape and pressure was applied to ensure good adhesion between fibers and tape. In order to reduce the possible coupling effect between the tape and the fiber bundle, we used tape only on one side of the fiber bundle. Sample testing length was 10 mm and width was 19 mm (the width of the tape).

0040-5175/$2.00

TABLE I. Specifications of the tested bundle.

Fiber type	PET	PP	Glass	Kevlar 49
Denier per fiber	3.33	5.14	3.26	1.55
Fibers per bundle	45	34	144	110
Fiber density, g/cm^3	1.36	0.91	2.54	1.45
Fiber initial modulus, GPa	2.4	2.9	72	130
Fiber tenacity, GPa	1.2	1.0	4.5	3.5
Fiber breaking strain, %	112.6	29.89	4.6	6.4

TABLE II. Specifications of the 3M Scotch 810 Magic Tape, as provided by the manufacturer.

Backing	Matte acetate
Adhesive	synthetic
Adhesion to steel	27.90 g/mm width
Tensile strehgth	242 g/mm width
Breaking strain	55.2%
Total width	19 mm
Thickness	0.635 mm

Each fiber bundle-tape assembly was prepared and tested at four different oblique angles, as shown in Figure 1, *i.e.*, $\theta = 0°$, 10°, 20°, and 30°. We found that for any angle greater than 30°, the fiber bundles could not be held securely in both clamps of the machine. Moreover, we anticipated that during extension of the specimens, the original oblique angle θ would change because of the elongation and the Poisson effect of the specimen, so that the actual oblique angle θ would be smaller.

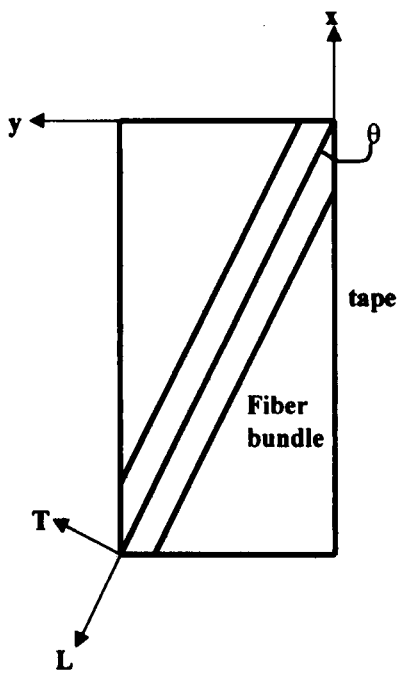

FIGURE 1. Prepared specimen and coordinate systems.

Prior to testing, all specimens were conditioned for at least 24 hours at 21°C and 65% RH for atmospheric equilibrium and sufficient fiber-tape curing so that the fibers bonded well to the tape. The testing was performed on an Instron. Specimens were well gripped by the clamps with no slippage. During testing, because of the short gauge length (10 mm), there were no noticeable ripples in the specimens.

The testing results at four different angles for four fiber types are provided in Tables III and IV, where Table III lists the specimen breaking loads and Table IV the specimen percentage breaking strains. Each data point is the average of at least 15 tests.

TABLE III. Tested bundle breaking load and SD values (in parantheses) at different obliquities.

θ	PET, Kg	PP, Kg	Glass, Kg	Kevlar, Kg
0°	6.34 (0.31)	5.83 (0.33)	8.32 (0.40)	8.16 (0.29)
10°	5.83 (0.39)	5.31 (0.24)	8.20 (0.30)	7.41 (0.36)
20°	5.81 (0.29)	5.50 (0.46)	7.98 (0.34)	6.87 (0.29)
30°	5.74 (0.20)	4.79 (1.29)	6.41 (0.54)	5.76 (0.28)

TABLE IV. Tested bundle breaking strains (%) and SD (in parantheses) values at different obliquities.

θ	PET	PP	Glass	Kevlar
0°	40.95 (6.55)	45.35 (8.35)	9.15 (0.60)	10.15 (0.71)
10°	38.75 (9.85)	34.80 (3.66)	10.65 (0.70)	11.10 (0.77)
20°	38.15 (5.95)	36.20 (10.51)	12.95 (1.31)	13.79 (1.04)
30°	38.00 (5.75)	29.20 (9.70)	15.50 (1.58)	15.73 (6.92)

Results and Analysis

We have assumed that changes in fiber obliquities do not significantly alter the nature of any possible fiber-tape coupling interactions, and as a result, tape strength and breaking strain can be treated as constant for specimens with different fiber obliquities.

Table III shows that when the oblique angle increases, the breaking loads for all specimens of four fiber types decrease. To explain this, some theoretical analysis is needed using Figure 1.

In the following analysis, we assume there is a state of uniform uniaxial stress in the samples. Given the low length-to-width aspect ratio of the samples, this assumption is a little crude. Consequently, conclusions drawn from the analysis will tend to be conservative or underestimated.

If we designate the fiber direction as L and the transverse direction as T, the loading direction as x and the direction perpendicular to the x direction as y, then the

stresses applied at the $x - y$ axes can be transformed to $L - T$ axes:

$$\begin{pmatrix} \sigma_L \\ \sigma_T \\ \tau_{LT} \end{pmatrix} = (T)\begin{pmatrix} \sigma_x \\ \sigma_y \\ \tau_{xy} \end{pmatrix} , \quad (1)$$

where the transformation matrix (T) for 2-D plane case is given by

$$(T) = \begin{pmatrix} \cos^2\theta & \sin^2\theta & 2\sin\theta\cos\theta \\ \sin^2\theta & \cos^2\theta & -2\sin\theta\cos\theta \\ -\sin\theta\cos\theta & \sin\theta\cos\theta & \cos^2\theta - \sin^2\theta \end{pmatrix}, \quad (2)$$

and θ is the oblique angle.

The stress-strain relationship at $L - T$ axes can then be expressed as

$$\begin{pmatrix} \sigma_L \\ \sigma_T \\ \tau_{LT} \end{pmatrix} = \begin{pmatrix} Q_{11} & Q_{12} & 0 \\ Q_{12} & Q_{22} & 0 \\ 0 & 0 & 2Q_{66} \end{pmatrix}\begin{pmatrix} \epsilon_L \\ \epsilon_T \\ 1/2\,\lambda_{LT} \end{pmatrix} , \quad (3)$$

where

$$Q_{11} = \frac{E_L}{1 - \nu_{LT}\nu_{TL}} , \quad (4)$$

$$Q_{22} = \frac{E_T}{1 - \nu_{LT}\nu_{TL}} , \quad (5)$$

$$Q_{12} = \frac{\nu_{LT}E_T}{1 - \nu_{LT}\nu_{TL}} = \frac{\nu_{TL}E_L}{1 - \nu_{LT}\nu_{TL}} , \quad (6)$$

$$Q_{66} = G_{LT} , \quad (7)$$

E_L and E_T are the elastic moduli of the specimen in the longitudinal and transverse directions, respectively, G_{LT} is the shear modulus, and ν_{LT} and ν_{TL} are major and minor Poisson ratios. Furthermore, in our present case where $\sigma_y = \tau_{xy} = 0$, the strains in the $L - T$ axes can be calculated directly from Equations 1 and 3 as

$$\epsilon_L = \frac{1}{E_L}(\cos^2\theta - \nu_{LT}\sin^2\theta)\sigma_x , \quad (8)$$

$$\epsilon_T = \frac{1}{E_T}(\sin^2\theta - \nu_{TL}\cos^2\theta)\sigma_x , \quad (9)$$

$$\lambda_{LT} = \frac{1}{G_{LT}}(\cos\theta\sin\theta)\sigma_x . \quad (10)$$

There are several theories we can use to predict the failure of the specimens. If we adopt the maximum strain failure theory [1], the three breaking strains are related to the three strengths by

$$\epsilon_{LU} = \frac{\sigma_{LU}}{E_L} , \quad (11)$$

$$\epsilon_{TU} = \frac{\sigma_{TU}}{E_T} , \quad (12)$$

and

$$\lambda_{LU} = \frac{\tau_{LTU}}{G_{LT}} , \quad (13)$$

where ϵ_{LU} and σ_{LU} are the breaking strain and tensile strength in the longitudinal direction, ϵ_{TU} and σ_{TU} are the breaking strain and tensile strength in the transverse direction, and λ_{LU} and τ_{LTU} are the shear breaking strain and shear strength. So the failure of the specimen will occur if the applied load σ_x exceeds the smallest of

$$\frac{\sigma_{LU}}{(\cos^2\theta - \nu_{LT}\sin^2\theta)} , \quad (14)$$

$$\frac{\sigma_{TU}}{(\sin^2\theta - \nu_{TL}\cos^2\theta)} , \quad (15)$$

and

$$\frac{\tau_{LTU}}{(\cos\theta\sin\theta)} . \quad (16)$$

Of the three criteria, when the oblique angle θ increases, the first criterion will lead to an increase in σ_x, and the second one will experience a change of load from compression when θ is small to tension when θ is large. Both are in conflict with the testing results in Table III, so the only criterion left is the shear strain term in the third criterion: when θ increases, the applied breaking load will decrease. This is consistent with the experimental results in Table III.

Fibers are best at carrying axial tension. However, Equation 16 reveals that when there is an oblique angle, a shear stress will be generated and exerted upon the fiber, and the shear strain, as indicated in Equation 10, will increase with the oblique angle. In light of the discussion above and the data in Table III, we can draw two conclusions. First, the shear strength is always the lowest in comparison with the longitudinal and transverse tensile strengths. Second, fibers are more vulnerable under shear stress. That explains why the yarn strength will decrease once the twist level is beyond the optimal level because of the increasing shear stress.

The change of breaking strain with θ, however, has different patterns for different fiber types; this is in general consistent with the conclusion of Hearle *et al.* [3]. More specifically, for brittle fibers such as glass and Kevlar specimens, the breaking strains increase with the oblique angle, opposite to the trend of the breaking load. But for ductile fibers, including PET and PP, breaking strains in general show a decreasing pattern consistent

with the breaking load. These two different patterns associated with fiber types need to be further explored.

Note that the breaking strain of the tape is greater than all the fibers, and the tape breaks later so as to ensure that the fiber bundles remain oblique prior to breaking during testing. The only exception is the PET fiber, which is undrawn and possesses a breaking strain much greater than the tape. Therefore, in this case, the data for PET specimens in Tables III and IV are the maximum values at the peak on the stress-strain curve, which is when the tape breaks before the PET fiber bundle. However, since all the data were taken at the same position, *i.e.*, the peak on the curve, they are still comparable and should not affect our conclusion.

As we reported previously [8], in a fiber-two-layer-tape structure, there were interactions between the fiber and tape during elongation, leading to the fragmentation phenomenon and a synergistic effect in the breaking load. That is, the breaking load of the fiber-tape system was greater than the sum of the tape and fibers. In the current test, the breaking strains of the specimens in Table IV are in general greater than those of the fibers, except in the case of PET, which as we mentioned above, had not broken when the data were taken. We carefully checked every link of the test, and found that the most plausible explanation for this increased breaking strain is again due to the interactions between fiber and tape, although we only used one piece of tape for each specimen. This raises the question of how to differentiate the effects due to fiber obliquity and those due to the fiber-tape interactions. Lacking further evidence, we have to assume, as mentioned before, that the fiber-tape interaction remains constant for different fiber obliquities, so that our conclusions are still valid. Further work is underway to verify our assumption of a constant fiber-tape interaction. Another potential problem is bonding quality between the fibers and the tape, which will have some influence on the results, but will probably not affect our general conclusions.

Furthermore, as we mentioned earlier, during the extension of the specimen, the original oblique angle θ will become smaller due to the elongation of the specimen and Poisson's ratio effect. Yet, this change of the oblique angle will not alter the value sequence of the angles for all the specimens, and therefore will not change our conclusions. The actual θ prior to specimen failure can be calculated, but the process is quite lengthy and the results add little useful information.

Finally, we must point out that this technique does not simulate the exact deformation of the fibers in three-dimensional helical orientation within a yarn. Fibers especially suffer torsional effects in a tensioned yarn because of the helical orientation, which is not represented in this test. Yet, it is conceivable that our conclusions will still be valid with the superposition of a torsional action on the specimen; this would likely intensify the severity of the loading on these specimens and magnify the changes we have observed here.

Conclusions

This work reveals that when fibers are tested off-axis, they become weaker because of the shear stress exerted on them. The shear strength of fibers is lowest in comparison with the longitudinal and transverse tensile strengths, and fibers are hence more vulnerable under shear stress.

The changing trends of breaking strain of the fibers, however, depend on the nature of fibers. For brittle fibers such as glass and Kevlar, the breaking strains increase with the oblique angle, opposite to the trend of breaking load. But for ductile fibers like PET and PP, breaking strains in general show a decreasing pattern consistent with the breaking load.

Readers should be aware that our technique does not simulate exactly the three-dimensional helical orientation of fibers within a yarn. However, our conclusions are still likely to be applicable to the helical orientation case, except that the severity of the loading on the fibers is intensified.

Literature Cited

1. Agarwal, B., and Broutman, L. J., "Analysis and Performance of Fiber Composites," 2nd ed., John Wiley & Sons, Inc., NY, 1990, p. 174.
2. Chang, B. W., Huang, P. H., and Smith, D. G., A Pinned-end Figure for Off-axis Testing, *Exp. Tech. (6), 28 (1984).*
3. Hearle, J. W. S., Grosberg, P., and Backer, S., "Structural Mechanics of Fibers, Yarns, and Fabrics," vol. 1 John Wiley & Sons, Inc., NY, 1969, pp. 232, 242.
4. Pipes, R. B., and Cole, B. W., On the Off-axis Strength Test for Anisotropic Materials, *J. Composite Mater.* **7,** 246 (1973).
5. Richards, G. L., Airhart, T. P., and Ashton, J. E., Off-axis Tensile Coupon Testing, *J. Composite Mater.* **3,** 586 (1969).
6. Sun, C. T., and Chung, I., An Oblique End-tab Design for Testing Off-axis Composite Specimens, *Composites* **24,** 619 (1993).
7. Sun, C. T., and Berreth, S. P., A New End Tab Design for Off-axis Tension Test of Composite Materials, *J. Composite Mater.* **3,** 766 (1988).
8. Wang, X., Zhang, Y., Postle, R., and Pan, N., An Experimental Examination on the Strength of Wool and Wool Reinforcement, in "Proc. 2nd China International Textile Conference," Xian China, 1998, p. 277.

Manuscript received April 16, 1999; accepted July 13, 1999.